Optics Communications 361 (2016) 148–152

Contents lists available at ScienceDirect

Optics Communications

journal homepage: www.elsevier.com/locate/optcom

Broadband terahertz anti-reflective structure fabricated by femtosecond laser drilling technique

Yibin Zhang [a], Minghui Yuan [a], Lin Chen [a,*], Bin Cai [a], Rui Yang [b], Yiming Zhu [a,*]

[a] Shanghai Key Lab of Modern Optical System, Engineering Research Center of Optical Instrument and System, Ministry of Education, University of Shanghai for Science and Technology, No. 516 JunGong Road, Shanghai, China
[b] BOCOM Smart Network Technologies, F18-20, Guangqi Mansion, No. 456, Hongcao Road, Shanghai, China

ARTICLE INFO

Article history:
Received 7 July 2015
Received in revised form
22 October 2015
Accepted 25 October 2015

Keywords:
Terahertz
Antireflection
Femtosecond laser
High-resistivity silicon

ABSTRACT

We fabricated several reverse conical holes on high-resistivity silicon substrate with different power and pulse number of femtosecond laser, and investigated their patterns and features by using scanning electron microscope (SEM). Then, we chose one of the experimental parameters prepared a reverse conical anti-reflection structure sample with period of 90 μm. Terahertz Time-domain Spectroscopy (THz-TDS) was used to test its properties. Compared with the nonstructural high-resistivity silicon, the transmission of structural high-resistivity silicon increases by the maximum of 14% in the range 0.32–1.30 THz. Furthermore, we simulated the sample by finite integral method (FIM). The simulated results show good consistency with experimental results. The transmission effect of the reverse conical holes were optimized via simulation. Results show that the related transmission effect can be improved by increasing the pulse numbers and decreasing the spot size of the femtosecond laser. The different transmission window can also be tuned by changing the reverse conical structure of different periods.

1. Instruction

In recent years, terahertz technology has attracted much more attentions in many scientific fields [1]. Terahertz components, such as resonant waveguides [2–4], filters [5,6], polarizers [7], sensors [8] and diodes [9], are necessary in various terahertz systems. For example, the high-resistivity silicon is usually utilized in Terahertz Time-domain Spectroscopy (THz-TDS) as a device which enables the transmission of terahertz wave while isolating the 800 nm femtosecond laser due to its high refractive index and broad transmission window (from microwave to mid-infrared wave). However, the high-resistivity silicon still gives rise to 30% loss because of Fresnel reflection, which will reduce dynamic range of THz-TDS. Hence, it is necessary to reduce reflective loss of high-resistivity silicon surface for further improving THz-TDS performance. There are two common methods to reduce the reflective loss. One is to coat thin film on high-resistivity silicon surface. This film should be single layer with the material of $n=(n_1 \cdot n_2)\hat{}1/2 \approx 1.85$ or multiple layers with materials of different refractive indices according to the film design theory [10–12]. Another is to fabricate micro-structure on silicon wafer. For instance, Huang et al. fabricated a biomimetic silicon nanotip (SiNTs) structure by utilizing self-masking dry etching technique. While the transmission refinement of the device was confined above 1 THz [13]. A bandwidth adjustable pyramid-based structure was built by Zhang et al. using a crystallographic wet etching method. Restricted by the fabrication method, the aspect-ratio of the device is unadjustable [14]. Brückner et al. utilized DRIE technique and fabricated two kinds of transmission enhancing structures (rectangle and hexagon). Although the amplitude of the electric field was enhanced by 15.2% and 21.76% independently, the fabrication period requires 7.2 h due to the 500 μm depth of the structures [15]. Other researchers fabricated sub-wavelength surface-relief structure on the basis of the zeroth-diffraction-order theory [16–19].

As is mentioned above, for realizing the later kind of transmission enhancing way, the common fabrication method are dry/wet etching. It is inconvenient for these methods to alter aspect ratio because of limitation of crystal orientation of wet etching [14] and limitation of etching speed and cost of dry etching [15]. Moreover, a lithography step is needed for realizing the periodic structures, which increases the complexity of the fabrication. In this paper, we abandoned the common dry/wet etching method and utilized the laser ablation technique to fabricate the transmission enhancing structure. This laser ablation method can realize controllable aspect-ratio as well as controllable bandwidth transmission structures in terahertz spectrum. This method have been proven to be useful in fabricating anti-reflection structures

* Corresponding authors. Fax: +86 21 33773176.
E-mail addresses: linchen@usst.edu.cn (L. Chen), ymzhu@usst.edu.cn (Y. Zhu).

http://dx.doi.org/10.1016/j.optcom.2015.10.051
0030-4018/

for visible light spectrum application [20,21].

According to the principle of interaction between femtosecond beam and silicon surface, we obtained the reverse conical holes with different diameters on the high-resistivity silicon surface by adjusting the power and pulse number of femtosecond laser. Then, we chose one of the experimental parameters, fabricated, experimentally and theoretically discussed the performance of the reverse conical anti-refraction sub-wavelength structure. The results show that the relative transmission of the structured sample increases by 14% at maximum in the range from 0.32 to 1.30 THz compared with the unstructured one. The different transmission window can be tuned by changing the reverse conical structure of different periods. Furthermore, the transmission effect of the sample can be improved by increasing the pulse numbers and decreasing the spot size of the femtosecond laser.

2. Experiments

Fig. 1 shows the setup of experiment. After the femtosecond laser beam with wavelength of 800 nm and power of 650 mW passes through beam splitter and shutter controller, it is focused on the silicon surface by lens with focal length of 200 mm. The silicon is fixed on a metal plate, which is controlled by step motor. By adjusting angle of beam splitter and switching time of shutter controller, the power and pulse number of femtosecond laser can be controlled.

In order to seek for proper experimental parameters, we obtained different patterns and features of holes fabricated on the high-resistivity silicon surface with different laser parameters. In the experiment, we chose the single side-polished silicon with resistivity of 20,000–28,000 Ω cm and crystal orientation of $<100>$ and fixed such 3×3 cm^2 silicon wafer on the metal plate. The position of metal plate was adjusted to ensure the silicon wafer being on the focal point of lens. The power of femtosecond laser and pulse number was arranged in 30–200 mW and 1000–6000 pulses, respectively. The average of holes diameters fabricated by different laser parameters is shown in Fig. 2. As we can see, the diameters of holes alter from 64 μm to 232 μm when the power of femtosecond laser increases and the trend accords with the Gaussian curve fitting results. Meanwhile, with the increase of femtosecond laser pulse number, the diameter decreases. The phenomenon can be explained by analyzing the SEM top view of sample. As shown in Fig. 3, we can see the center of the conical hole became darker and darker as the number of laser pulse increases. There are lots of residues around holes which generated by the interaction between the femtosecond laser beam and silicon surface and its quantity depends on the volume of the holes. When the pulse number of laser increases, the depths of holes and the generated residues also increase. It is the residue surrounding holes that gradually accumulates and extrudes, and finally causes the decrease of holes diameters. As a result, the diameter and depth of holes can be changed by altering the power and the pulse number of femtosecond laser, respectively.

In Fig. 2, the diameter of constructed hole was 93 μm when the power and pulse number was set to 50 mW and 3000 pulses, respectively. In order to fabricate a compact sample, we set the step

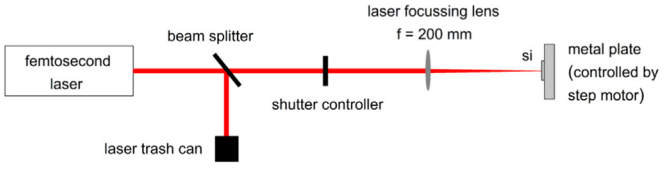

Fig. 1. The sketch of experiment set.

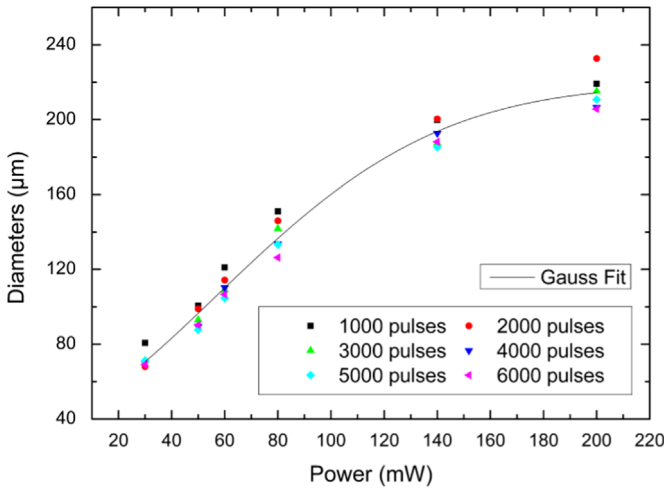

Fig. 2. The fitting results of hole diameter versus different laser power and pulse numbers.

of step motor to 90 μm, which is relative to the diameter. Then, the sample with array holes on silicon was fabricated, which is shown in Fig. 4. From Fig. 4(a), we can see the silicon surface has high quality periodical structure. Here we focus on its anti-reflective feature. From cross section as shown in Fig. 4(b), we can see the surface is rough and the tip of cone is a bit crooked. The depth of inverse cone is roughly 130 μm.

3. Measurements and simulation

The Fiber Coupled Terahertz Time Domain Spectrometer was used in the experiment and the polarization of THz wave was kept paralleled with the direction of period. The result (red line) is shown in Fig. 5. As comparison, we also listed the experiment results of unstructured silicon (blue line). There are three obvious peaks in THz time domain spectrum, the first peak is signal, the other peaks are reflection peaks, which caused by muti-reflection of signal in silicon. The When we see the frequency spectrum in Fig. 5(b), the signal of structured silicon is higher than unstructured silicon in the range from 0.32 to 1.30 THz (the transmission window width is 0.98 THz). The relative transmission ($T=P_{\text{structured}}/P_{\text{unstructured}}$, Fig. 7) increases by 14% at the maximum (about 0.81 THz).

To understand the anti-reflection mechanism of reverse conical structure, we adopt the graded index method to analyze it. As shown in Fig. 6(a) and (b), we consider the reverse conical structure with period of 90 μm and depth of 130 μm as combination of infinite layers with different refractive indices n_i, The n_i of each layer can be determined by the effective refractive index formula as following:

$$n_{eff} = \sqrt{(1-\alpha)n_1^2 + \alpha\, n_2^2} \tag{1}$$

where n_1 and n_2 are the refractive indices of air and silicon, α is the filling factor (area fraction) of silicon in each layer [22]. As shown in Fig. 6(b), if we use the vertical distance of each layer to silicon surface x, the filling factor α can be expressed as:

$$\alpha = 1 - \frac{\pi}{4}\times\left(1-\frac{x}{L}\right)^2 \tag{2}$$

where L is the height of entire reverse conical structure. By substituting Eq. (2) into Eq. (1), the filling factors α of different vertical distances x can be obtained as red dash in Fig. 6. It can be clearly seen that the effective refractive index curve increases

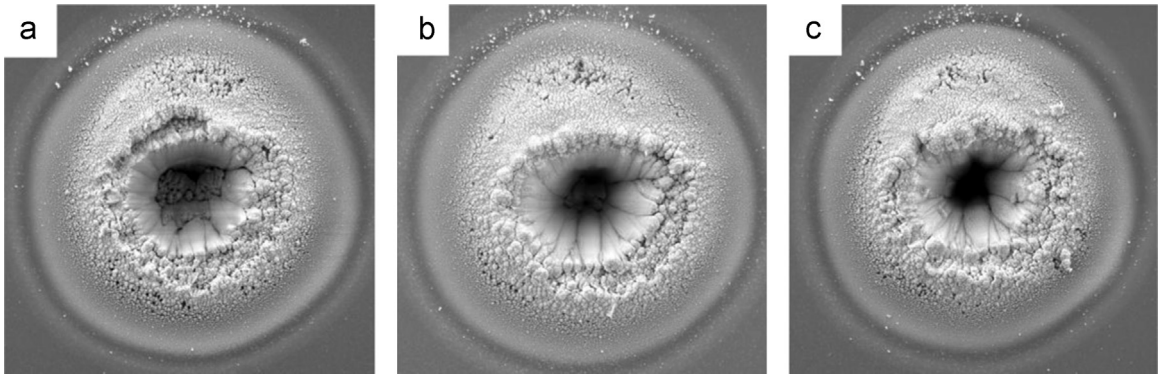

Fig. 3. The top view of unit reverse conical hole by SEM: (a) laser power=30 mW and pulse number=2000 pulses, (b) laser power=30 mW and pulse number=3000 pulses, (c) laser power=30 mW and pulse number=4000 pulses.

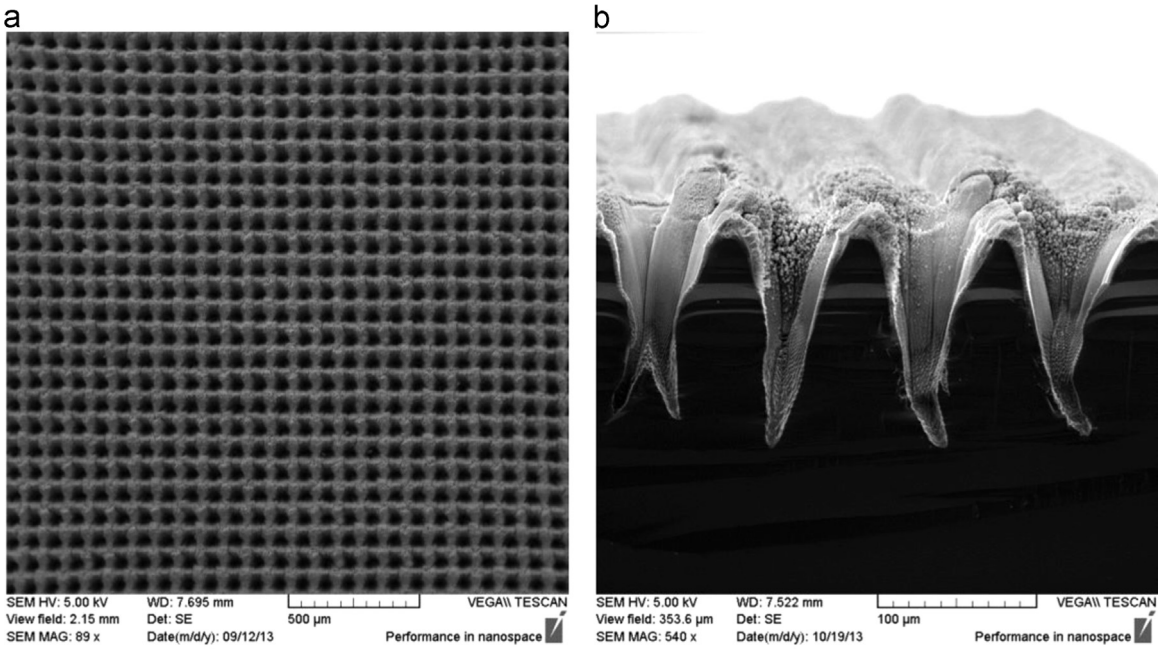

Fig. 4. The (a) top view and (b) cross section of sub-wavelength structure of period being 90 μm on high-resistivity silicon wafer by SEM.

continuously with vertical distances x increases. According to Fresnel formula: $t=2n_2/(n_1+n_2)$, when the refractive indices of adjacent layers n_1 and n_2 are extremely close to each other [23], the transmission of incident electromagnetic wave is nearly 100%. Hence, it is feasible that reverse conical structure can enhance the transmission of high-resistivity silicon although a part of energy will lose because of suddenly change of the refractive index n from 1 to 1.85 on the silicon wafer surface.

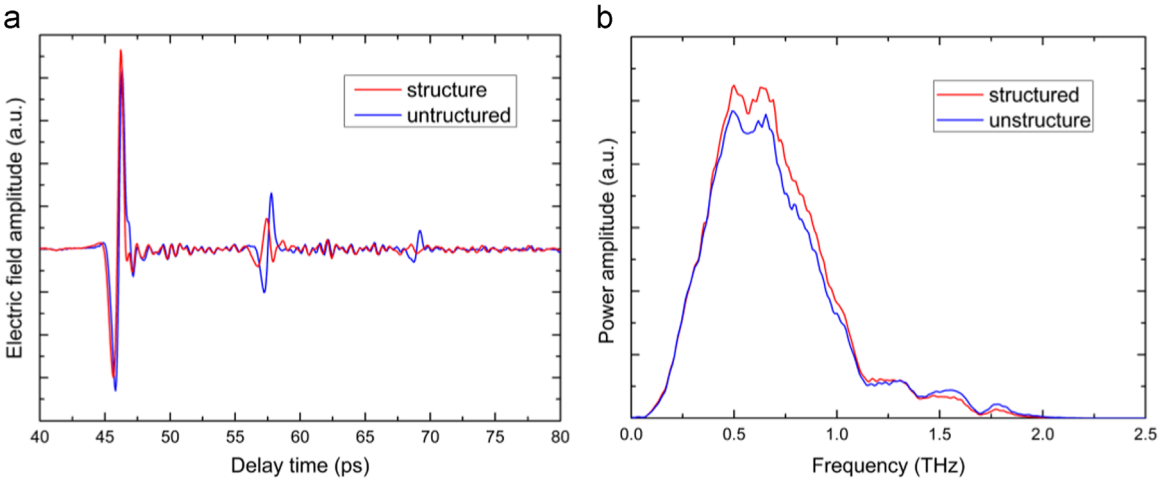

Fig. 5. The (a) time domain signal and (b) frequency domain spectrum of reverse conical structure sample.

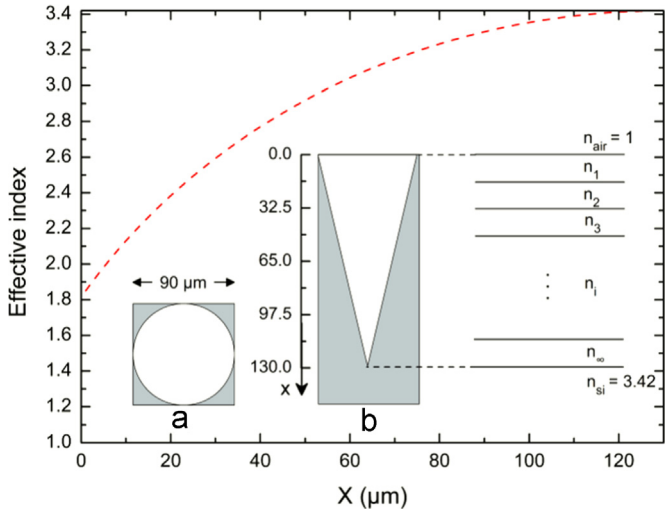

Fig. 6. The sketch of unit reverse conical structure and the effective index of different vertical distance *x*.

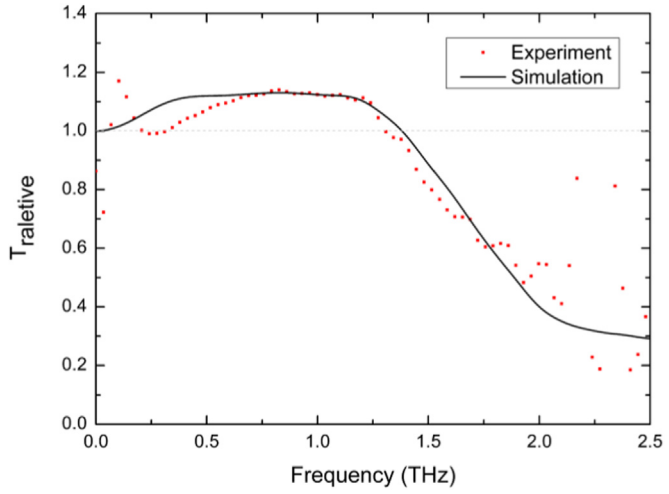

Fig. 7. The experimental and simulated results of same reverse conical structure.

We consider the reverse conical structure shown in Fig. 4 to be the ideal reverse conical structure shown in Fig. 6(a) and (b), and use CST Microwave Studio with time domain solver based on finite integral method (FIM) to simulate the structure. The simulated transmission of reverse conical structure (solid line) is show in Fig. 7. It can be clearly seen that the relative transmission increases, flattens and then decreases with the varying of frequency, which accorded with the experimental data (red dotted line) except it is a bit higher than the experimental results before 0.7 THz. This mismatch might be caused by the structural difference between the experiment and the simulation.

Next, the relation is discussed between period and transmission window width. Based on the zeroth-diffraction-order theory, the period of grating and passable frequency are subject to [15]:

$$f \le \frac{c}{\Lambda}\cdot\frac{f_g}{n_i \sin\theta_i \cos\varphi + (n_s^2 + n_i^2 \sin^2\theta_i \sin^2\varphi)^{1/2}} \quad (3)$$

When the period of grating changes, the cut-off frequency also changes. Thus, we can alter the period of reverse conical structure to alter the location of cut-off frequency as well as the transmission window width. As shown in Fig. 8, we simulate the ideal reverse conical structures with different periods (60–180 μm) but same depth-to-width ratio (13:9) by CST Microwave Studio. The results point out the transmission window widths with different

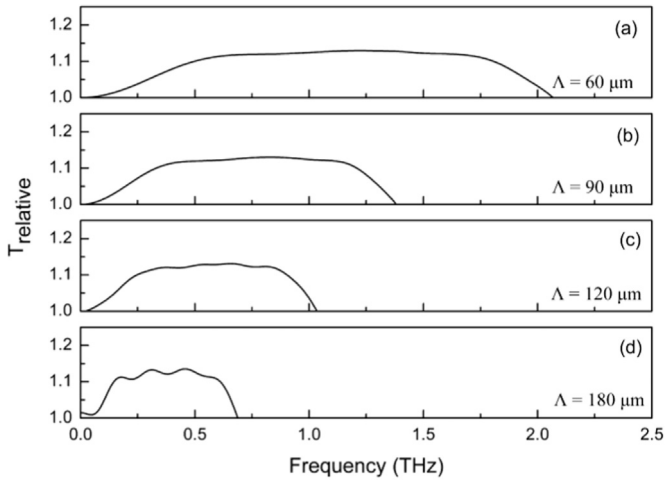

Fig. 8. The simulation results of reverse conical structure on different periods (60–180 μm) but same depth-to-width ratio (13:9).

periods of 60, 90, 120 and 180 μm are 2.07, 1.38, 1.04 and 0.69 THz respectively. Their maxima transmission remains constant at the value of 1.13. Moreover, it can be seen from Fig. 8 that the cut-off frequency of the device decreases as the periodic number increases. The reason will be explained in the following part.

To improve the transmission effect of the sample, we did research on relation between the transmission spectrum and the aspect ratio, simulation is performed on periodic number and depth of the ideal reverse conic structures independently. As shown in Fig. 9(a), the transmission window of 130 μm in depth reverse conical structures (with periodic number of 60, 90, 120 and 180 μm) are 2.34, 1.38, 0.94 and 0.56 THz, independently. Results show that the transmission window becomes wider as the periodic number decreases. Moreover, the curves in Fig. 9(a) have the same low cut-off frequency and ascending tendency. As a result, it can be inferred that the variation of low cut-off frequency in Fig. 8 is due to the change of the conic depth. As shown in Fig. 9(b), the deeper the height is, the smaller the low cut-off frequency become. The transmission window of 45, 90, 180 and 450 μm in height reverse conical structures (with aspect-ratio of 0.5, 1, 2, and 5) are 1.05, 1.22, 1.54 and 1.49 THz, independently. The maximum transmission bandwidth is achieved when the depth and periodic number of the inverse conical structures reach 180 μm and 2, independently. Results show that the by increasing the conic depth (aspect-ratio) adequately, the transmission bandwidth can be widened effectively. Based on the results of Fig. 8 and Fig. 9(b), increasing the aspect-ratio of the structures is benefit for improving its terahertz transmission ability. As the aspect-ratio reaches 5, the transmission peak reaches ~1.18. It can be concluded that for achieving a wide bandwidth terahertz transmission structure, the periodic number should be small and the aspect-ratio should be high. In our experiments, the reverse conical structure samples of different periods mentioned above can be realized by changing the power and pulse number of femtosecond laser. Besides, we also can consciously increase the depth of reverse conical structure to raise the depth-to-width ratio by enhancing the pulse numbers of femtosecond laser. The period of sample is limited by the size of focused laser spot.

4. Conclusion

The reverse conical structures of different diameters (64–232 μm) were obtained on high-resistivity silicon by employing the femtosecond laser of different power (30–200 mW) and

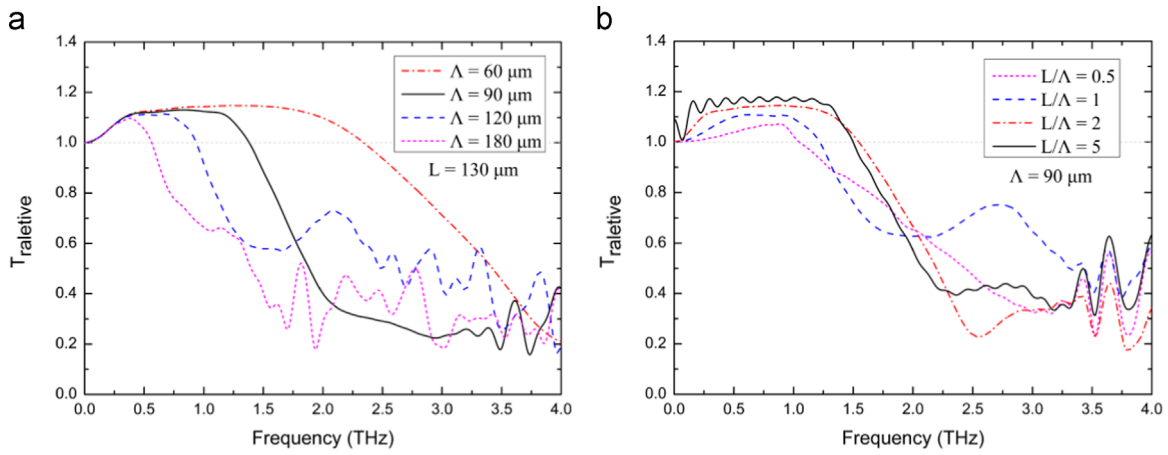

Fig. 9. Simulated results of reverse conical structures with different depth and period: (a) depth: 130 μm, period: 60, 90, 120 and 180 μm, independently. (b) period: 90 μm, depth: 45, 90, 180 and 450 μm, independently.

different pulse numbers (1000–6000 pulses). Then we chose the power and pulse number as 50 mW and 3000 pulses, respectively, to prepared a reverse conical anti-reflection structure sample with period of 90 μm. The relative transmission of this sample increases by 14% at maximum in the range from 0.32 to 1.30 THz compared with the unstructured one. The simulated results on same structure accord with the experimental data. We also did further simulations on different periods (60–180 μm) but same depth-to-width ratio (13:9) on the basis of this fact. The simulations show that it is feasible to adjust the transmission window width by change the power and pulse number of femtosecond laser. Furthermore, the transmission effect of the reverse conical holes were optimized via simulation. Results show that the related transmission effect can be improved by increasing the pulse numbers and decreasing the spot size of the femtosecond laser. In consideration of influence of error of fabrication and diameter of laser spot, the optimization of transmission of structure still has amounts of work to do, which will be further discussed in our future work.

Acknowledgment

This work was partly supported by the National Program on Key Basic Research Project of China (973 Program, 2014CB339806), Basic Research Key Project (12JC1407100), Major National Development Project of Scientific Instrument and Equipment (2011YQ150021) (2012YQ14000504), National Natural Science Foundation of China (11174207) (61138001) (61205094) (61307126), Shanghai Rising-Star Program (14QA1403100), Program of Shanghai Subject Chief Scientist (14XD1403000), Hujiang Foundation of China (C14002), Zhejiang Key Discipline of Instrument Science and Technology (JL150505), and the New Century Excellent Talents Project from the Ministry of Education (NCET-12-1052).

Reference

[1] M. Tonouchi, Cutting-edge terahertz technology, Nat. Photonics 1 (2007) 97–105.
[2] L. Chen, C.M. Gao, J.M. Xu, X.F. Zang, B. Cai, Y.M. Zhu, Observation of electromagnetically induced transparency like transmission in terahertz asymmetric waveguide-cavities systems, Opt. Lett. 38 (2013) 1379–1381.
[3] L. Chen, J.M. Xu, C.M. Gao, X.F. Zang, B. Cai, Y.M. Zhu, Manipulating terahertz electromagnetic induced transparency through parallel plate waveguide cavities, Appl. Phys. Lett. 103 (2013) 251105.
[4] L. Chen, Z.X. Cheng, J.M. Xu, X.F. Zang, B. Cai, Y.M. Zhu, Controllable multiband terahertz notch filter based on a parallel plate waveguide with a single deep groove, Opt. Lett. 39 (2014) 4541–4544.
[5] L. Chen, Y.M. Zhu, X.F. Zang, B. Cai, Z. Li, L. Xie, S.L. Zhuang, Mode splitting transmission effect of surface wave excitation through a metal hole array, Light Sci. Appl. 2 (2013) e60.
[6] L. Chen, K.V. Truong, Z.X. Cheng, Z. Li, Y.M. Zhu, Characterization of photonic bands in metal photonic crystal slabs, Opt. Commun. 333 (2014) 232–236.
[7] L.Q. Cong, N.N. Xu, W.L. Zhang, R.J. Singh, Polarization Control in terahertz metasurfaces with the lowest order rotational symmetry, Adv. Opt. Mater. (2015).
[8] R.J. Singh, W. Cao, I. Al-Naib, L.Q. Cong, W. Withayachumnankul, W.L. Zhang, Ultrasensitive terahertz sensing with high-Q fano resonances in metasurfaces, Appl. Phys. Lett. 105 (2014) 171101.
[9] Q. Li, Z. Tian, X.Q. Zhang, R.J. Singh, L.L. Du, J.Q. Gu, J.G. Han, W.L. Zhang, Active graphene-silicon hybrid diode for terahertz waves, Nat. Commun. 6 (2015).
[10] I. Hosako, Multilayer optical thin films for use at terahertz frequencies: method of fabrication, Appl, Optics 44 (2005) 3769–3773.
[11] D. Poitras, J.A. Dobrowolski, Toward perfect antireflection coatings. 2. Theory, Appl. Opt. 43 (2004) 1286–1295.
[12] Withawat Withayachumnankul, Bernd M. Fischer, Samuel P. Mickan, Derek Abbott, Retrofittable antireflection coatings for T-rays, Microw. Opt. Technol. Lett. 49 (2007) 2267–2270.
[13] Y.F. Huang, S. Chattopadhyay, Y.J. Jen, C.Y. Peng, T.A. Lin, Y.K. Hsu, C.L. Pan, H. C. Lo, C.H. Hsu, Y.H. Chang, C.S. Lee, K.H. Chen, L.C. Chen, Improved broadband and quasi-omnidirectional anti-reflection properties with biomimetic silicon nanostructures, Nat. Nanotechnol. 2 (2007) 770–774.
[14] Y.W. Chen, P.Y. Han, X.C. Zhang, Tunable broadband antireflection structures for silicon at terahertz frequency, Appl. Phys. Lett. 94 (2009) 041106.
[15] C. BrüRckner, T. Känsebier, B. Pradarutti, S. Riehemann, G. Notni, E.B. Kley, A. Tünnermann, Broadband antireflective structures applied to high resistive float zone silicon in the THz spectral range, Opt. Express 17 (2009) 3063–3077.
[16] C. Brückner, B. Pradarutti, O. Stenzel, R. Steinkopf, S. Riehemann, G. Notni, A. Tünnermann, Broadband antireflective surface-relief structure for THz optics, Opt. Express 15 (2007) 779–789.
[17] S. Kuroo, K. Shiraishi, H. Sasho, H. Yoda, K. Muro, Triangular surface-relief grating for reduction of reflection from silicon surface in the 0.1–3 THz region, in: Proceedings on the Conference on Lasers and Electro-Optics, 2008, Opt. Soc. Am., CThD7.
[18] A. Thoman, A. Kern, H. Helm, M. Walther, Nanostructured gold films as broadband terahertz antireflection coatings, Phys. Rev. B 77 (2008) 195405.
[19] Shin-ichi Kuroo, Satoshi Oyama, Kazuo Shiraishi, Hiroyuki Sasho, Kazushiro Fukushima, Reduction of light reflection at silicon-plate surfaces by means of subwavelength gratings in terahertz region, Appl. Opt. 49 (2010) 2806–2812.
[20] Jing Yang, Fangfang Luo, Tsung Sheng Kao, Xiong Li, Ghim Wei Ho, Jinghua Teng, Xiangang Luo, Minghui Hong, Design and fabrication of broadband ultralow reflectivity black Si surfaces by laser micro/nanoprocessing, Light: Sci. Appl. 3 (2014) e185.
[21] A.Y. Vorobyev, Chunlei Guo, Antireflection effect of femtosecond laser-induced periodic surface structures on silicon, Opt. Express 19 (2011) A1031–A1036.
[22] L. Escoubas, J.J. Simon, M. Loli, G. Berginc, F. Flory, H. Giovannini, An antireflective silicon grating working in the resonance domain for the near infrared spectral region, Opt. Commun. 226 (2003) 81–88.
[23] L. Chen, Z.Q. Cao, F. Ou, H.G. Li, Q.S. Shen, H.C. Qiao, Observation of large positive and negative lateral shifts of a reflected beam from symmetrical metal-cladding waveguides, Opt. Lett. 32 (2007) 1432–1434.